

Category-specific integration of homeostatic signals in caudal but not rostral human insula

W Kyle Simmons¹⁻³, Kristina M Rapuano³, Seth J Kallman³, John E Ingeholm³, Bernard Miller⁴, Stephen J Gotts³, Jason A Avery^{1,5}, Kevin D Hall⁴ & Alex Martin³

Prevailing theories hold that the insula is functionally organized along its caudal-to-rostral axis, with posterior regions coding lower-level sensory information and anterior regions coding higher-level stimulus significance relative to the body's homeostatic needs. Contrary to predictions of this model, the response of the taste-sensitive region of the caudal, but not rostral, insula to food images was directly related to the body's homeostatic state as indexed by levels of peripheral glucose.

It is widely held that there exists along the insula a caudal-to-rostral functional organization, with more caudal regions representing primarily lower-level sensory interoceptive, gustatory and somatosensory signals, and rostral regions contributing to higher-level cognition and emotion by integrating information about the body's homeostatic state with information represented in limbic and executive control networks^{1,2}. Although the neuroanatomical connections between the insula and the peripheral nervous system suggest that homeostatic integration occurs in more caudal insular regions, particularly in the mid-insula where gustatory and visceral information from cranial nerves VII, IX and X first reaches the cerebral cortex via subcortical projections through the brainstem and thalamus³, it is also frequently asserted that anterior insula integrates this homeostatic information about the state of the body with higher cognitive functions.

A direct empirical test of the prevailing account within a single group of individuals would require identifying a sensory stimulus that activates both rostral and caudal regions of the insular cortex and then demonstrating (i) that the rostral, but not caudal, region is involved in higher-level cognition related to that sensory modality and (ii) that the rostral region's response reflects the current state of homeostatic signals. We have identified a set of stimuli and tasks that satisfy these requirements.

The human neuroimaging literature demonstrates the existence of multiple insular gustatory areas, including primary gustatory cortex located caudally in the dorsal mid-insula as well as a rostral insula gustatory region^{4,5}. Several human functional imaging studies also have demonstrated that viewing pictures of food activates regions

of the insula⁶⁻⁹. Although it has been assumed that these activations reflect the automatic retrieval of conceptual information about taste⁶, whether any region of insula cortex responds to both pictures of food and gustatory stimuli has yet to be demonstrated. According to the prevailing model of insular functional organization, one might expect that (i) more caudal (sensory) gustatory cortex would not be engaged in higher-level conceptual cognition related to food pictures, whereas (ii) the more rostral gustatory cortex would be engaged by viewing pictures of food, but it would do so in a manner that integrates information from homeostatic signals that are relevant to this object category. As the primary index of immediately available energy resources for both the body and brain, circulating glucose levels would seem to be the homeostatic marker most directly related to food object perception¹⁰. As such, the prevailing theory of insula functional organization predicts that whereas the caudal insular gustatory cortex should not respond differently to food images relative to non-food images, the rostral insular gustatory cortex responses to food, relative to non-food, images should be greater when circulating glucose levels are low and lower when circulating glucose levels are high.

To test these predictions, we asked 21 right-handed healthy adults (8 male, age range 23–39 years) to perform a food versus non-food

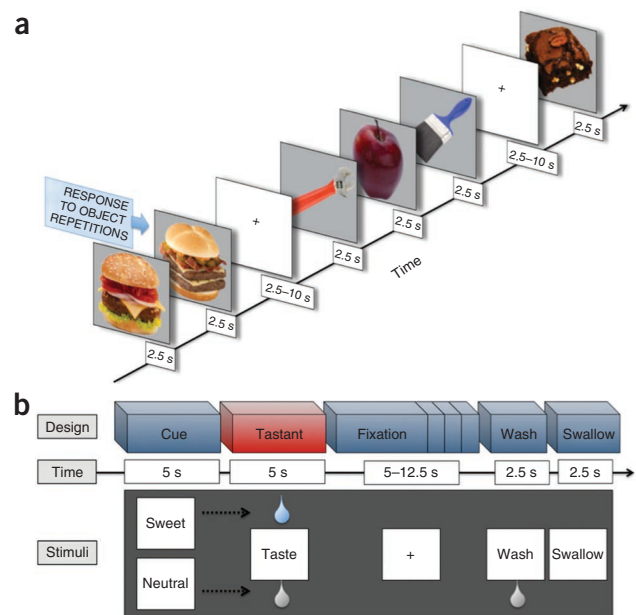


Figure 1 fMRI task descriptions. (a) Food versus non-food picture-repetition detection task. (b) Single trial in the gustatory mapping task. See Online Methods for detailed task descriptions.

¹Laureate Institute for Brain Research, Tulsa, Oklahoma, USA. ²Faculty of Community Medicine, The University of Tulsa, Tulsa, Oklahoma, USA. ³Laboratory of Brain and Cognition, National Institute of Mental Health (NIMH), National Institutes of Health (NIH), Bethesda, Maryland, USA. ⁴Laboratory of Biological Modeling, National Institute of Diabetes and Digestive and Kidney Diseases (NIDDK), NIH, Bethesda, Maryland, USA. ⁵Department of Biological Science, The University of Tulsa, Tulsa, Oklahoma, USA. Correspondence should be addressed to W.K.S. (wksimmons@laureateinstitute.org).

Received 30 May; accepted 5 September; published online 29 September 2013; doi:10.1038/nn.3535

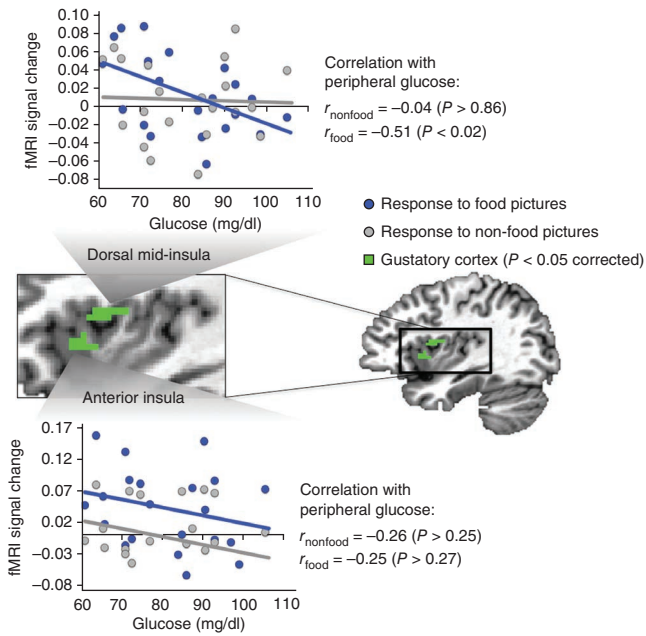


Figure 2 Insula gustatory cortex responses to food and non-food pictures as a function of circulating glucose level. The anterior insula gustatory cortex exhibited overall greater responses to food than non-food images. In the dorsal mid-insula, however, the response to food, but not non-food, images was modulated by peripheral glucose.

picture-repetition detection task while undergoing functional magnetic resonance imaging (fMRI) (Fig. 1a and Supplementary Fig. 1). Importantly, blood was drawn from each subject immediately before he or she performed the task and assayed for plasma glucose levels. Immediately after the food versus non-food picture task and while still in the scanner, subjects underwent a gustatory mapping task in which a magnetic resonance-compatible tastant delivery system was used to deliver tastants and tasteless control solutions (Fig. 1b).

The gustatory mapping task identified two regions within the left insula where activity was significantly greater in response to the tastant (Fig. 2), one located more caudally in the dorsal mid-insula and another located more rostrally in the anterior insula. Both regions have been previously identified as gustatory cortex via meta-analysis⁵.

Within the rostral anterior insula taste-responsive region, activity was greater when subjects viewed food pictures than when they viewed non-food pictures, $t(20) = 2.93$, $P < 0.009$. This is the first demonstration of an insula region responsive to both food images and tastants; however, activity in response to food and non-food images was not reliably related to peripheral glucose levels ($r_{\text{food}} = -0.25$, $P > 0.27$; $r_{\text{nonfood}} = -0.26$, $P > 0.25$; Fig. 2), and neither was the difference in activity between food and nonfood images ($r_{\text{difference}} = 0.01$, $P > 0.96$; Supplementary Fig. 2). In contrast, peripheral blood glucose levels significantly modulated the response of the more caudal dorsal mid-insula to food images ($r = -0.51$, $P < 0.02$) but not non-food images ($r = -0.04$, $P > 0.86$). Notably, the category specificity of this effect is demonstrated by the reliable association between circulating glucose and the difference in the region's responses to food and non-food images ($r_{\text{difference}} = -0.49$, $P < 0.03$; Supplementary Fig. 2).

This finding directly contradicts prevailing assumptions about insula functional organization^{1,2}, which would predict integration between the body's homeostatic state and higher cognitive (conceptual) processing in the rostral insula, and a lack of conceptual food category-specific activity in more caudal mid-insula gustatory cortex. Although rostral

insula taste cortex was indeed sensitive to the conceptual category of pictured food objects, it did not show sensitivity to information about the body's homeostatic state. Rather, we found that it was the mid-insular gustatory cortex that showed homeostatically sensitive conceptual category-specific responses. The neuroanatomical connectivity of this region certainly supports this type of integration, as the dorsal mid-insula is known to have connections through the thalamus to one of the primary central nervous system sites for peripheral glucodetection, located in the nucleus of the solitary tract^{3,11,12}.

Along with the results of other recent studies challenging prevailing assumptions about the insula^{13–16}, the present findings provide an empirical challenge to the view that moving rostrally along the insula is necessarily associated with greater integration of the body's homeostatic state and higher cognitive processing. This finding will require new thinking about the relative roles of the rostral versus caudal portions of the insula. One possible division of labor suggested by our results is that the rostral insula plays a role in maintaining stable conceptual representations of food categories, whereas the more caudal mid-insula permits contextual flexibility depending on the current state of the body.

METHODS

Methods and any associated references are available in the online version of the paper.

Note: Any Supplementary Information and Source Data files are available in the online version of the paper.

ACKNOWLEDGMENTS

We would like to thank K. Burrows for help with data management and analysis of the high-sweetness and low-sweetness food pictures. This research supported by the Intramural Research Programs of the NIMH and the NIDDK, as well as by NIMH grant K01MH096175-01 to W.K.S., a grant from the Oklahoma Center for the Advancement of Science and Technology (OCAST HR10-141) to W.K.S., a NARSAD Young Investigator Award to W.K.S., a grant to W.K.S. from the Oklahoma Tobacco Research Center, and The William K. Warren Foundation. The study was conducted under NIH Clinical Study Protocol 09-DK-0081 (ClinicalTrials.gov ID NCT00846040).

AUTHOR CONTRIBUTIONS

W.K.S. designed and conducted the experiments, contributed to data analysis and wrote the manuscript. K.M.R. and S.J.K. conducted the experiments and contributed to data analysis. J.E.I. contributed to the construction of equipment for the study and conducted the experiment. B.M. conducted the experiment and contributed to interpreting metabolic data. S.J.G. contributed to data analysis and writing the manuscript. J.A.A. contributed to writing the manuscript, and K.D.H. and A.M. helped design the experiment and contributed to writing the manuscript.

COMPETING FINANCIAL INTERESTS

The authors declare no competing financial interests.

Reprints and permissions information is available online at <http://www.nature.com/reprints/index.html>.

- Craig, A.D.B. *Nat. Rev. Neurosci.* **10**, 59–70 (2009).
- Craig, A.D.B. *Ann. NY Acad. Sci.* **1225**, 72–82 (2011).
- Craig, A.D. *Nat. Rev. Neurosci.* **3**, 655–666 (2002).
- Small, D.M. *Brain Struct. Funct.* **214**, 551–561 (2010).
- Veldhuizen, M.G. *et al. Hum. Brain Mapp.* **32**, 2256–2266 (2011).
- Simmons, W.K., Martin, A. & Barsalou, L.W. *Cereb. Cortex* **15**, 1602–1608 (2005).
- van der Laan, L.N., de Ridder, D.T.D., Viergever, M.A. & Smeets, P.A.M. *Neuroimage* **55**, 296–303 (2011).
- LaBar, K.S. *et al. Behav. Neurosci.* **115**, 493–500 (2001).
- Killgore, W.D., Young, A., Femia, L. & Bogorodzki, P. *Neuroimage* **19**, 1381–1394 (2003).
- Grayson, B.E., Seeley, R.J. & Sandoval, D.A. *Nat. Rev. Neurosci.* **14**, 24–37 (2013).
- Yettefti, K., Orsini, J.C. & Perrin, J. *Physiol. Behav.* **61**, 93–100 (1997).
- Beckstead, R.M., Morse, J.R. & Norgren, R. *J. Comp. Neurol.* **190**, 259–282 (1980).
- Khalsa, S.S., Rudrauf, D., Feinstein, J. & Tranel, D. *Nat. Neurosci.* **12**, 1494–1496 (2009).
- Damasio, A., Damasio, H. & Tranel, D. *Cereb. Cortex* **23**, 833–846 (2013).
- Philippi, C.L. *et al. PLoS ONE* **7**, e38413 (2012).
- Feinstein, J.S. *et al. J. Clin. Exp. Neuropsychol.* **32**, 88–106 (2010).

ONLINE METHODS

Subjects. Twenty-one healthy, native-English-speaking volunteers from the greater Washington, DC metropolitan area participated in this study for monetary compensation (8 male, age range 23–39 years). All participants were right-handed. Participants were excluded if they were obese; the average body mass index (BMI) was 22 kg/m² (range 18–28). Subjects were evaluated for psychiatric illness (including depression, anxiety and eating disorders) by a clinical psychologist and excluded if they currently, or had ever, met criteria for an axis I psychiatric diagnosis. Subjects were also excluded if they reported strict dietary concerns (for example, vegan diet) or involvement in regular, vigorous exercise regimens, or if they reported either daily use of alcohol or tobacco or the use of illicit drugs at any time in the preceding 6 months. Those with endocrine diseases (such as diabetes) or who were taking medications that could influence metabolism were also deemed ineligible. Screening included blood draws to assess blood lipid profile, liver panel, electrolytes and blood count, in addition to an electrocardiogram (EKG) and resting metabolic rate testing to determine eligibility. In addition to a non-obese BMI, subjects were required to have a stable weight, defined by a loss or gain of no more than 5 kg over the preceding 6 months. All subjects signed an informed consent form describing appropriate procedures and potential risks in accordance with the procedures specified by an NIH Institutional Review Board.

Experimental design. All subjects were entered as inpatients at the National Institutes of Health Clinical Center for at least 96 h before scanning and were provided a controlled diet ensuring that they were in a eucaloric state at the time of participation. While inpatient, subjects received an energy balanced diet (50% carbohydrate, 35% fat and 15% protein). Each participant's total caloric intake was based on 3-d diet and activity records, resting metabolic rate and body size measurements made during subject screening. At noon on the day of scanning, each subject was provided a meal standardized for macronutrient content. One hour and forty-five minutes later (at 13:45 h), blood was drawn from the subject's arm using standard venipuncture (see **Supplementary Fig. 1**). Immediately after the blood draw, subjects entered the scanner at 14:00 h and first performed the food/non-food picture-repetition detection task, followed immediately thereafter by the gustatory mapping task.

Food/non-food picture-repetition detection task. Subjects were presented pictures of food and non-food objects while undergoing fMRI. A broad selection of food stimuli was presented, including images of appetizing foods high in both fat and sugar content, as well as many healthy food options such as fruits and vegetables. One hundred and eighty distinct food pictures were presented over the course of the study. Forty-five distinct non-food object pictures were also presented. The non-food object pictures depicted common household and office tools (for example, pliers, hammers, staplers, etc.). A separate group of 12 adults who were not involved in the fMRI experiment participated in a stimulus-norming study to collect naming accuracy scores and typicality ratings for the food and non-food object pictures. Typicality was scored on a 1–7 scale, with “1” indicating that a particular object was not at all typical of the basic-level category it was meant to represent (i.e., banana, hamburger, pliers, stapler, etc.) and “7” indicating that the object was an extremely typical depiction of its basic-level category. Food and non-food picture naming accuracy was nearly identical (mean food naming accuracy = 99.1% (s.d. = 0.04%), mean non-food naming accuracy = 99.6% (s.d. = 0.02%), $P > 0.38$) and the pictures were found to be equally typical of their respective basic-level category (mean food typicality = 5.08 (s.d. = 0.68), mean non-food typicality = 5.09 (s.d. = 0.86), $P > 0.94$).

During fMRI, all photographs were presented for 2.5 s each in a pseudo-random order optimized for fMRI by optseq2 (<http://surfer.nmr.mgh.harvard.edu/optseq/>). Subjects were instructed to press a button only when two consecutive photographs depicted objects with the same name (for example, two consecutive cheeseburger images), and as such required only basic-level conceptual object naming. During the interstimulus intervals, a fixation cross appeared for varying durations (range 2.5–12.5 s). Each of the 3 scanning runs for the food/non-food picture-repetition detection task lasted 5 min and 17 s.

Gustatory mapping task. ‘Sweet’ and ‘neutral’ tastants were each made in four solutions of varying intensities. The sweet solutions, made with apple juice, were diluted concentrations of 25% and 50% juice, 100% juice and 100% juice

concentrated with the addition of 4 g of standard table sugar. Neutral solutions were varying dilutions (25%, 50%, 75% or 100%) of an artificial ‘saliva’ consisting of 25 mM (1.9 mg/mL) potassium chloride and 2.5 mM (210 mcg/mL) sodium bicarbonate. Prior to scanning, subjects underwent taste tests to determine which two of these eight liquids would be used in the scanner. During the taste test, each solution was administered three times, in random orders. Subjects rated tastes based on pleasantness, unpleasantness, intensity and sweetness. The averages of these three ratings were used to find the least intense ‘neutral’ and the most pleasant ‘sweet’ solution, while minimizing unpleasantness (and pleasantness for the neutral tastant). The neutral solution was also used as a ‘wash’ during the scan, though the subject was not explicitly told these were the same solutions.

Respective tastants were administered to the subjects through an MR-compatible, pneumatic-pressurized tastant-delivery system. The delivery of tastants to the subjects' mouths through the tastant delivery system was controlled via the National Instruments LabVIEW graphical programming environment. Liquids were released downwards from syringes through latex-free hospital-grade plastic tubing into a gustatory manifold attached to the head coil and adjusted to fit into the subject's mouth.

While in the scanner, subjects viewed single words that informed them of the sequence of events as they progressed. Subjects experienced three types of trials. Tastant trials displayed a cue (the word “sweet” or “neutral”) for 5 s, followed by the word “taste” for 5 s, at which point the subject received 0.4 ml of the respective tastant. Subjects were instructed to let the taste roll down on the tongue, but not to swallow. A fixation cross subsequently followed and remained on the screen for a variable amount of time (range = 2.5–12.5 s). Subjects were instructed to keep the tastant in their mouth and not swallow. Next, the word “wash” appeared for 2.5 s, and the subject was administered 0.8 ml of the neutral solution. After this, the word “swallow” appeared for 2.5 s, and the subject was instructed to then swallow both the tastant and the wash. There were 9 sweet taste and 9 neutral trials per run. Catch trials also occurred periodically, with the cue (“sweet” or “neutral”) appearing on the screen for 5 s, but without subsequently delivery of the tastant. Six “sweet” and six “neutral” catch trials occurred in each run. Finally, freestanding wash trials were also given by administering the tasteless (neutral) solution while displaying the “wash” cue for 2.5 s. The word “swallow” subsequently appeared for 2.5 s, after which the trial ended. During the interstimulus intervals subjects were shown a fixation cross for variable durations (range = 2.5–10 s). Each of the four gustatory mapping task scanning runs lasted 10 min and 20 s. In post-scan ratings, subjects reported that they experienced the sweet solution as having a significantly more intense taste than the tasteless solution (mean sweet = 50.5 (s.d. = 17.1), mean neutral = 15.5 (s.d. = 16.3); $t(13) = 6.722$, $P < 0.0001$).

Glucose measurements. Blood samples were collected into tubes containing EDTA and aprotinin as preservatives. All samples were kept on ice and then centrifuged (1,600g for 10 min at 4 °C) within 30 min of collection for isolation of plasma. After centrifugation, the plasma was immediately frozen and stored at –80 °C for later analysis. CLIA-certified glucose measurements were performed by the hexokinase method in the NIH Clinical Center Department of Laboratory Medicine.

Using this assay, the samples' mean circulating glucose levels was 81.2 mg/dl (s.d. = 12.9 mg/dl). **Figure 2** and **Supplementary Figures 2** and **3** display the distribution of glucose across the sample. Importantly, the amount of variation in the sample was sufficient to allow us to detect an association with insula activity.

Immediately before scanning, subjects completed measures indicating their level of hunger (0 = no hunger, 10 = extremely hungry) and sensations of fullness (0 = not at all full, 10 = very full). Hunger ratings were generally low (mean = 2.6, s.d. = 2.4), with fullness ratings near the middle of the scale (mean = 4.9, s.d. = 3.2). Significantly, neither of these ratings was significantly related to circulating glucose levels ($r_{\text{hunger}} = 0.14$, $P > 0.54$; $r_{\text{fullness}} = 0.24$, $P > 0.28$). Additionally, neither hunger nor fullness ratings correlated with food category-specific activity in either the anterior or dorsal-mid insula (mid-insula $r_{\text{hunger}} = -0.23$, $P > 0.32$; mid-insula $r_{\text{fullness}} = -0.05$, $P > 0.82$; anterior insula $r_{\text{hunger}} = -0.36$, $P > 0.15$; anterior insula $r_{\text{fullness}} = 0.06$, $P > 0.79$). This is important because in addition to gustatory inputs, the insula also receives visceral interoceptive information related to hunger and stomach distension³. The lack of association between the hunger/fullness ratings on the one hand,

and glucose and insula region of interest (ROI) activity on the other hand, thus strongly suggests that any relationships observed between circulating glucose and insula activity are not due instead to modulation of insula activity by visceral interoceptive information.

MRI data acquisition. All visual stimuli were presented via Eprime software (www.pstnet.com/). Stimuli were projected onto a screen in the scanner bore behind the subject's head and viewed through a mirror mounted to the head coil.

During the food/non-food picture-repetition detection task, 139 echoplanar magnetic resonance (MR) volumes were acquired with a 3T General Electric scanner and a Nova 16-channel receive-only head coil. Each echoplanar image (EPI) consisted of 44 2.8-mm slices (echo time (TE) = 27 ms, repetition time (TR) = 2,500 ms, flip angle = 90 degrees, voxel size = $3.4375 \times 3.4375 \times 2.8$ mm). Scan parameters for the gustatory mapping task runs were identical, except that 248 volumes were collected in each scanning run. High-resolution anatomical images were also collected (TE = 2.7 ms, TR = 7.24 ms, flip angle = 12 degrees, voxel size = $0.937 \times 0.937 \times 1.2$ mm). All structural and functional images were collected with a sensitivity encoding (SENSE) factor of 2, used to reduce image collection time (for structural images) or minimize image distortions (in functional images) while reducing gradient-coil heating over the course of the scan session.

fMRI pre-processing. Magnetic resonance imaging data were preprocessed and analyzed using the AFNI software package. Anatomical scans were spatially normalized to the Talairach and Tournoux standard space using AFNI's automated algorithm. The resulting spatial transformation parameters were then applied to the functional data. All functional volumes were aligned to the third volume taken in the first functional scanning run. For each subject, all scanning run time course files were visually inspected for quality control, and outlying time points caused by residual motion after image registration were censored out of the subsequent statistical analyses. All volumes were slice-time corrected and smoothed with a 6-mm full-width half-maximum Gaussian kernel. Finally, the signal for each functional voxel was normalized to the percent signal change from the voxel's mean across the scanning run's signal time-course.

Statistical analyses. For the food/non-food picture-repetition detection task, multiple regression was used at the single-subject level to estimate the response to each condition after accounting for covariates of non-interest. The regression model included regressors of non-interest for each run's signal mean, linear, quadratic and cubic signal trends, as well as the 6 motion parameters (3 translations and 3 rotations) recorded from image registration during preprocessing. The presentations of food and non-food images were modeled separately by a gamma variate function beginning at the onset of picture stimulus from each object category. A whole-brain group random effects paired-sample *t*-test corrected at $P < 0.05$ using the false discovery rate method revealed that relative to viewing non-food objects, viewing food images resulted in greater activity bilaterally in the anterior insula. Food images were also associated with greater activity bilaterally in the orbitofrontal cortex, dorsolateral prefrontal cortex, caudate, cuneus and fusiform gyrus. Additionally, food picture-related activity was observed in the right amygdala, left ventral striatum and thalamus. In contrast, relative to food images, non-food pictures bilaterally activated a region of middle temporal gyrus implicated in the perception of tool stimuli and non-biological motion^{17,18}.

The single-subject analysis of the gustatory mapping task also employed multiple regression. The regression model accounted for each run's signal mean, linear, quadratic and cubic signal trends as well as for the 6 motion parameters (3 translations and 3 rotations) recorded from image registration during preprocessing. Regressors were constructed to account for the presentation of "sweet" and "neutral" cue stimuli separately by convolving a box-car function of 5-s width beginning at the onset of each type of word cue with a gamma-variate function to adjust for the delay and shape of the blood oxygen level-dependent (BOLD) response. Additionally, a regressor was constructed to account for the wash/swallow events by convolving a box-car function of 5-s width beginning at the onset of the word "wash" with a gamma-variate function. Finally, presentations of sweet and neutral tastants were separately modeled by a gamma variate function beginning at the onset of the sweet and neutral stimuli. Gustatory mapping data were unavailable for

seven subjects because of either excessive head motion or complications with stimulus presentation.

Group random effects analysis of the gustatory mapping task used a paired-sample *t*-test comparing the subjects' regression coefficient (beta) maps for responses to sweet and neutral tastants. The resulting *t*-map was corrected for multiple comparisons at the $P < 0.05$ level using cluster-size corrections implemented via Monte Carlo simulations in AFNI's 3dClustSim. The insula is well known to be the location of gustatory cortex in humans. We therefore implemented a small volume correction within the insula, with a voxel-wise $P < 0.0025$ and cluster size threshold of 20 contiguous voxels to achieve correction for multiple comparisons at $P < 0.05$. We chose a voxel-wise threshold of $P < 0.0025$, rather than the more typical $P < 0.005$ used in many small volume corrections, because this threshold both was more stringent and identified two distinct gustatory-responsive regions of the left insula that closely resemble those identified in a recent meta-analysis of gustatory stimulation imaging studies⁵ (**Supplementary Table 1**). One region was located in the dorsal mid-insula near the fundus of the superior circular insular sulcus at the intersection of the insula and the overlying operculum, a region identified in previous research to be the location of human primary gustatory cortex^{4,19}. The second left insula region where activity was greater for the sweet taste versus the neutral tastant was located along the left anterior short insular gyrus, approximately 13 mm rostral and inferior to the left dorsal mid-insula cluster. As they were both located in the same hemisphere, these two regions served as good sites of comparison in testing the caudal-to-rostral account of insula functional organization. As reported here, ROI analyses were subsequently performed to determine whether these gustatory regions responded to food pictures and whether circulating glucose levels modulated the response to food pictures. Regarding sample size, the number of subjects in the study ($N = 21$) is greater than is typically the case in published fMRI studies, and research suggests that even approximately 20 participants per group in fMRI studies yields group activation maps that are consistent with larger sample size studies^{20,21}.

Additionally, a third taste-responsive region was also observed in the right mid-insula. Although this region in the right mid-insula exhibited a qualitatively similar association between peripheral glucose and responses to food images, but not non-food images, the effect did not reach statistical significance ($r_{\text{food}} = -0.27, P > 0.24$; $r_{\text{nonfood}} = -0.09, P > 0.70$). The region in the right mid-insula did, however, exhibit an overall greater response to food than non-food pictures ($t(20) = 2.93, P < 0.009$). The differences in the strength of the effects between the left and right hemispheres observed in the present study may be a fruitful avenue for future research. Various authors have noted that the two hemispheres may differ in their relative representation of sympathetic and parasympathetic interoceptive information^{22,23}, with the left hemisphere being relatively more engaged with parasympathetic activity. It thus may be that the stronger left hemisphere responses reported here are due to the fact that the current study used stimuli related to gustation and feeding that are associated with energy acquisition and enrichment, which are functions of the parasympathetic system. No regions in the insula exhibited greater responses to the neutral tastant.

In addition, before performing the study, we asked a group of adult participants who were not involved in the imaging experiment to classify the food pictures according to their sweetness. We used these ratings to separate the stimuli into "high sweet" and "low sweet" stimulus sets, and then compared the food category-specific response to each class (for example, high sweet versus non-foods, low sweet versus non-foods) as a function of glucose levels (**Supplementary Fig. 3**).

17. Beauchamp, M.S., Lee, K.E., Haxby, J.V. & Martin, A. *Neuron* **34**, 149–159 (2002).
18. Simmons, W.K. & Martin, A. *Soc. Cogn. Affect. Neurosci.* **7**, 467–475 (2012).
19. Veldhuizen, M.G., Bender, G., Constable, R.T. & Small, D.M. *Chem. Senses* **32**, 569–581 (2007).
20. Murphy, K. & Garavan, H. *Neuroimage* **22**, 879–885 (2004).
21. Friston, K. *Neuroimage* **61**, 1300–1310 (2012).
22. Wittling, W., Block, A., Genzel, S. & Schweiger, E. *Neuropsychologia* **36**, 461–468 (1998).
23. Craig, A.D.B. *Trends Cogn. Sci.* **9**, 566–571 (2005).